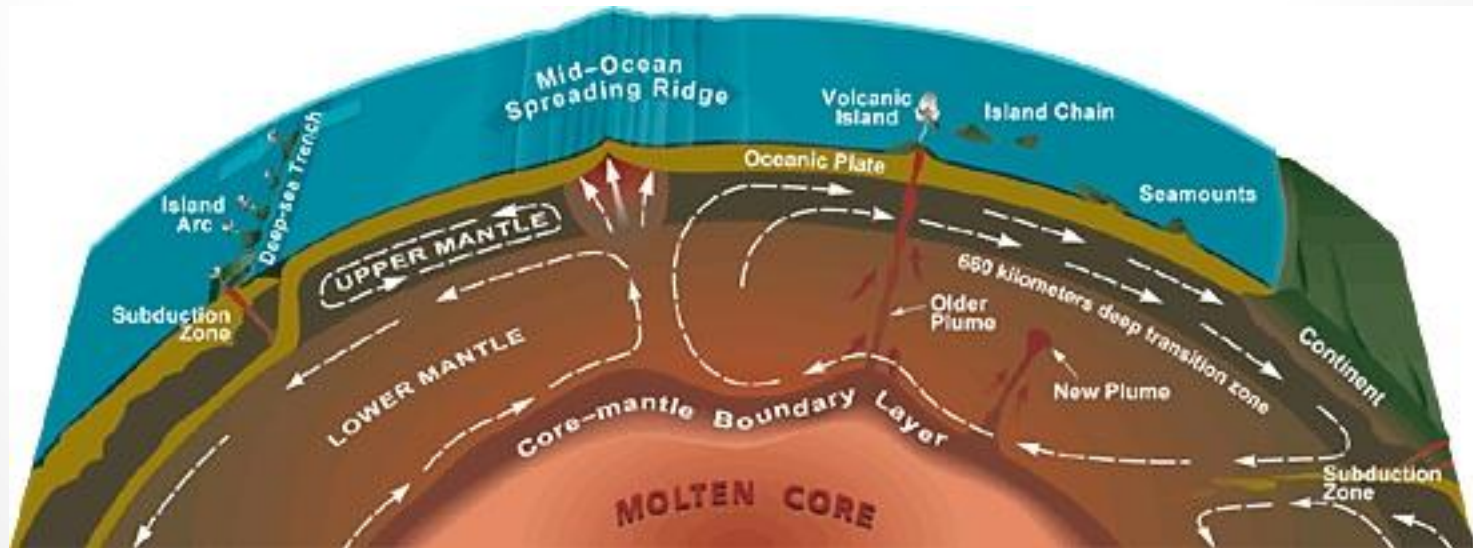
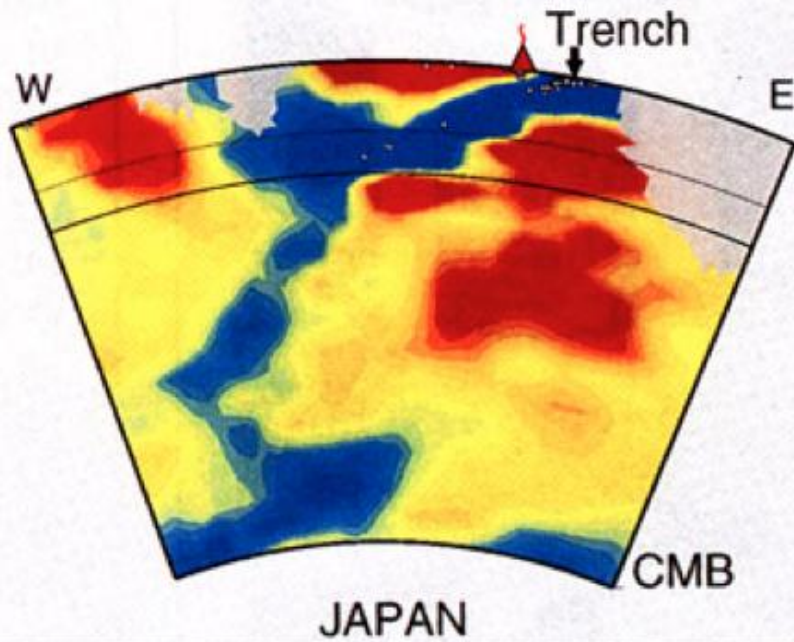


Whole Mantle Convection



Overview

1. Evidence for whole mantle convection
2. Model of whole mantle convection reconciling geophysical and geochemical data – Transition Zone Water Filter Model
3. Evidence for the Transition Zone Water Filter Model

Seismic Tomography from Grand (1997)

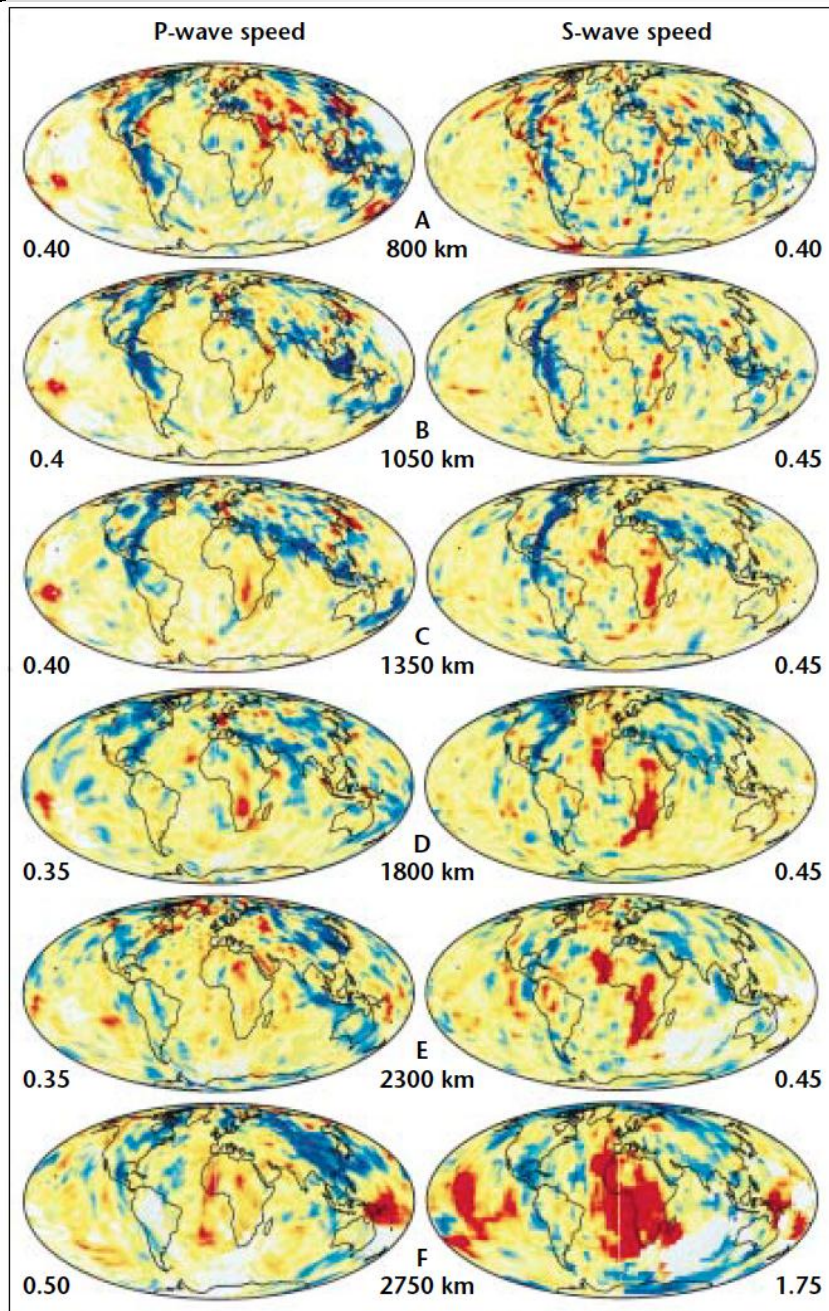
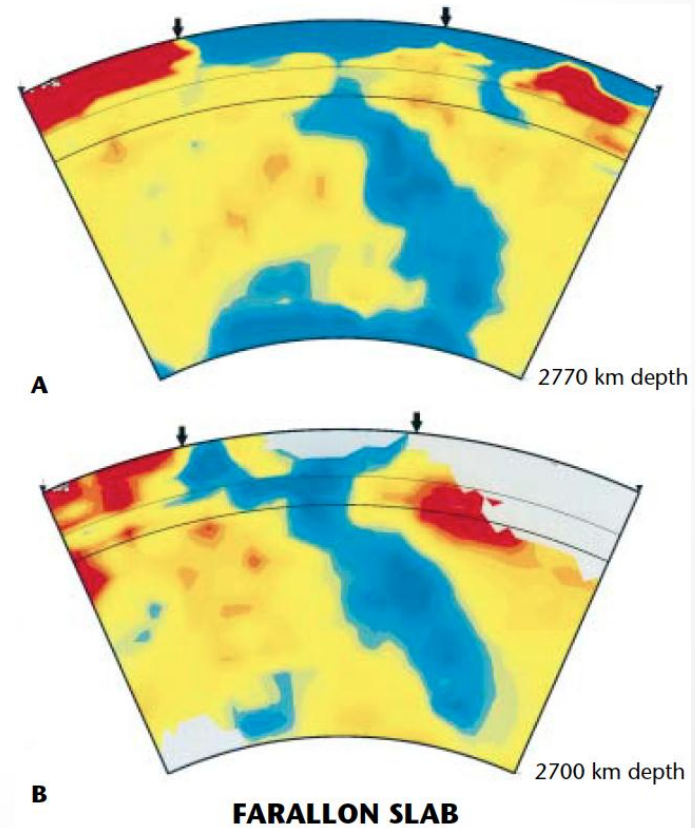


Figure 2. Comparison of P- and S-wave models, showing variations in seismic velocity at given depths through the lower mantle. Numbers at the sides of the images are the maximum anomaly in terms of percentage difference from mean velocity. Blue indicates faster than average, and red indicates slower than average. The white regions have no significant data sampling.



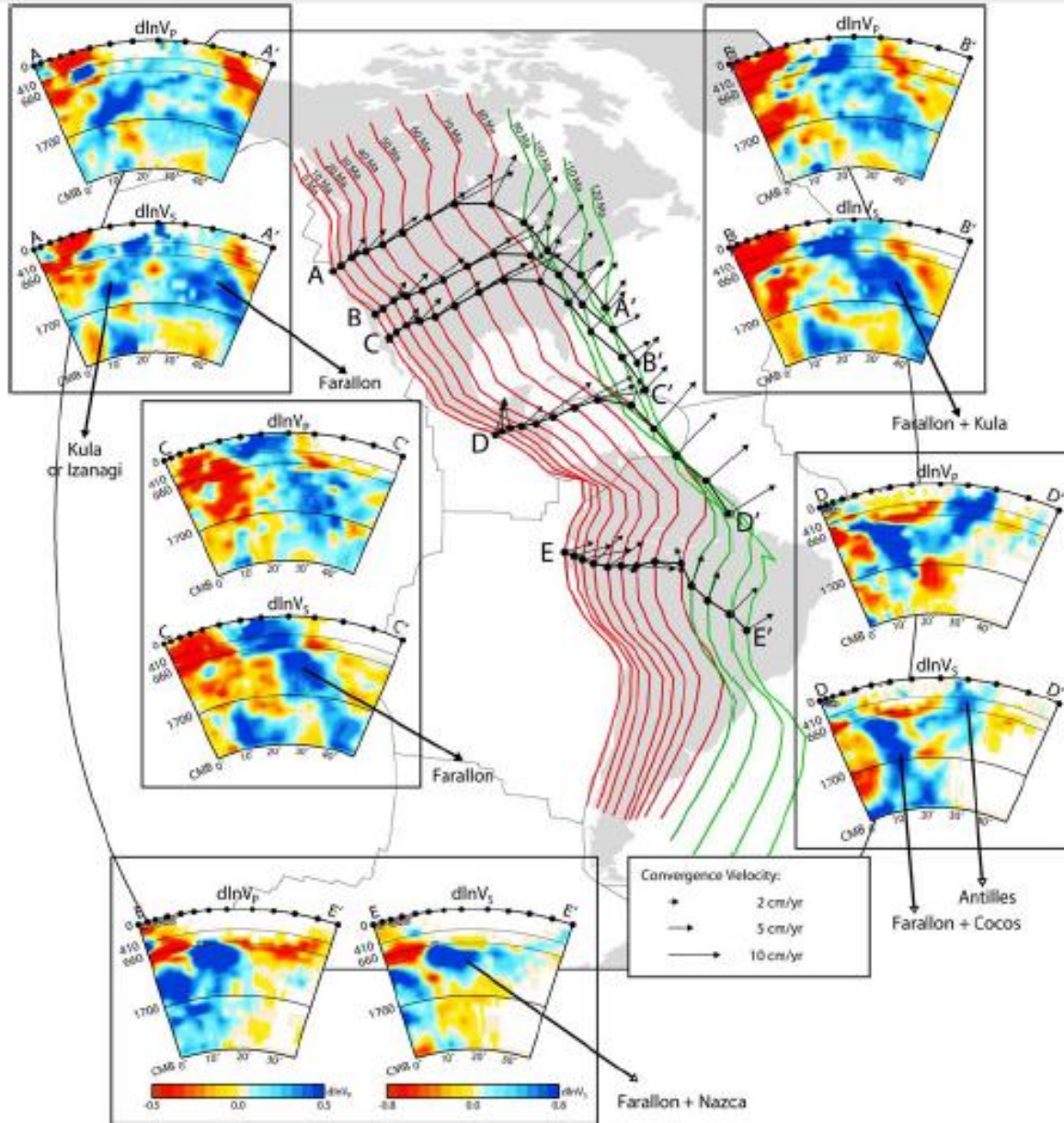


Figure 6. Cross sections through the model for P and S wave velocities. Red and green lines represent past boundary positions between Pacific seafloor and American continents since 120 Myr (computed from present boundary positions with rotation poles data in the hot spots reference frame). Black lines represent different cross sections made in our V_p and V_s models; different points along the lines represent past margin positions between 120 Myr and 0 Myr ago for given points in the present-day. Arrows represent velocities and directions of convergence at different ages, computed in the hot spots reference frame.

Imaging individual subducted slabs

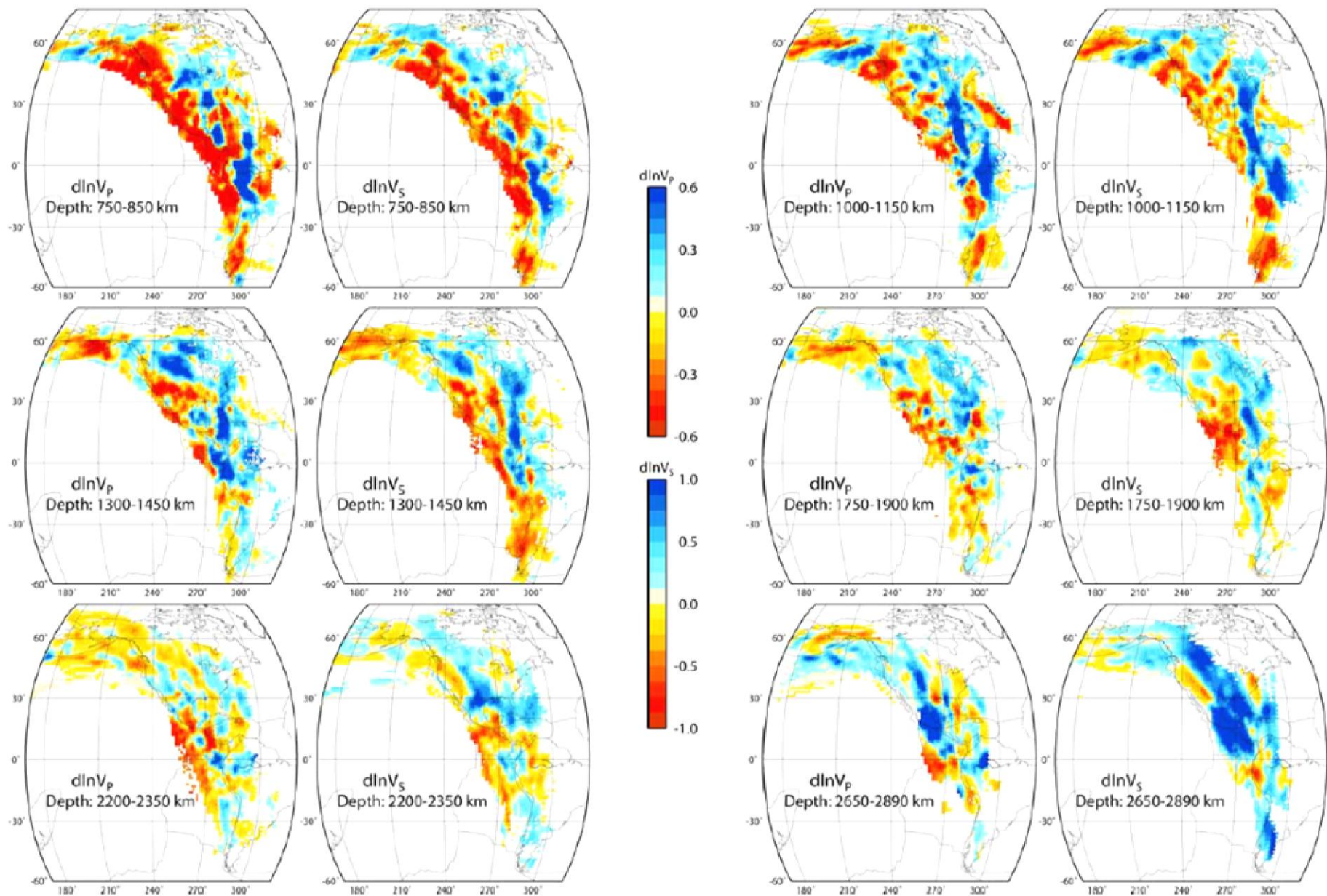
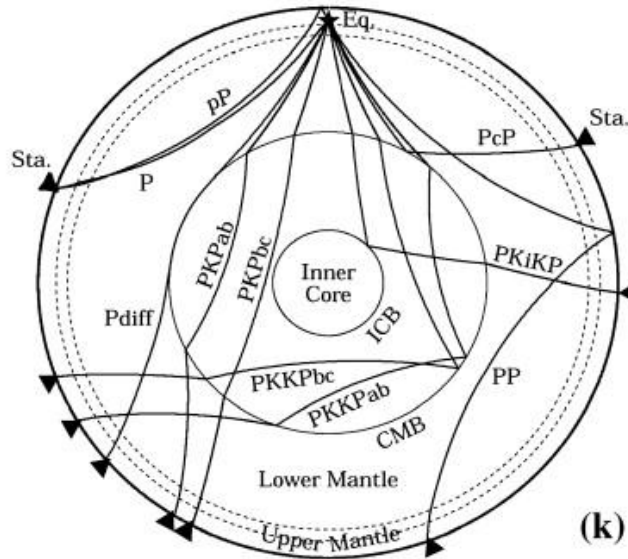
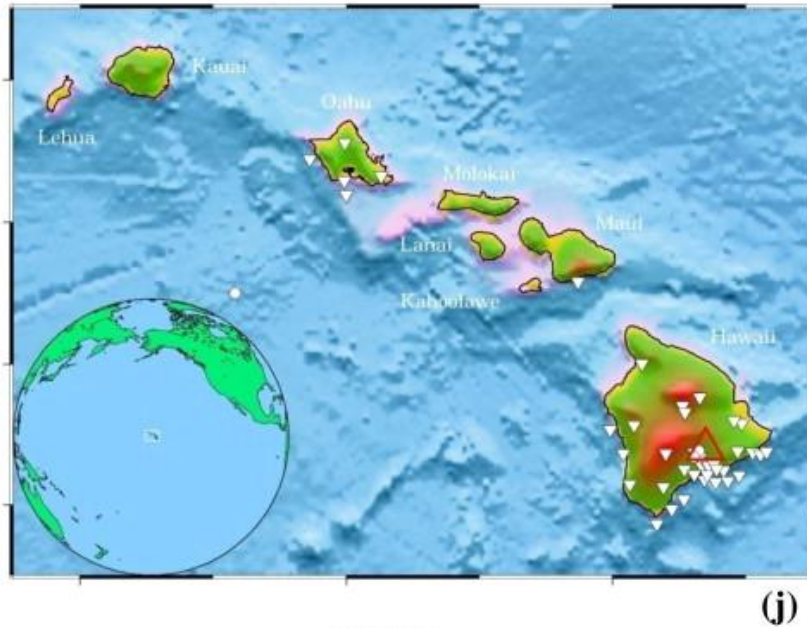
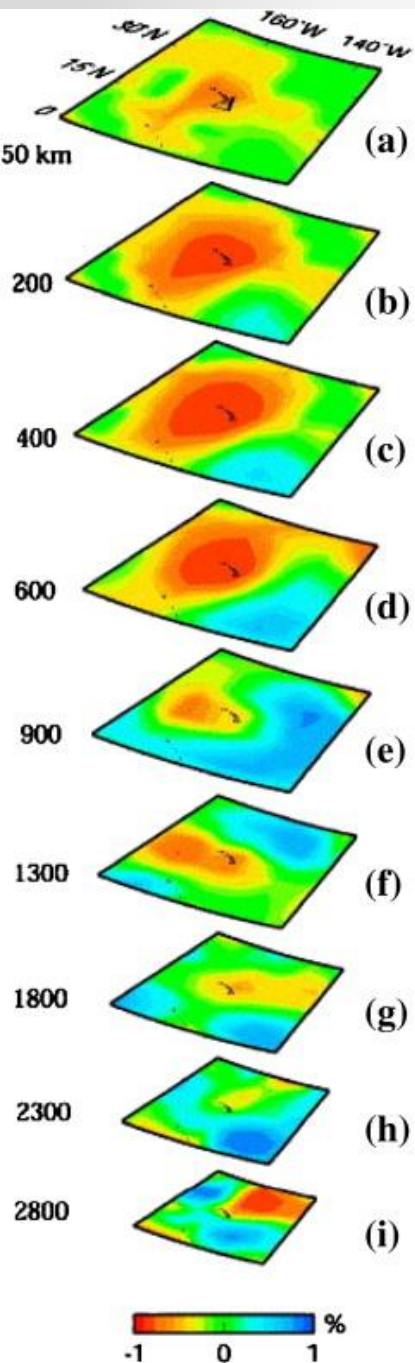


Figure 5. P wave and S wave velocity perturbation maps with respect to the ak135 reference model in the layers: 750–850 km, 1000–1150 km, 1300–1450 km, 1750–1900 km, 2200–2350 km, and 2650–2890 km. Cells that are not resolved are left white.



Imaging Hotspots Using Seismic Tomography

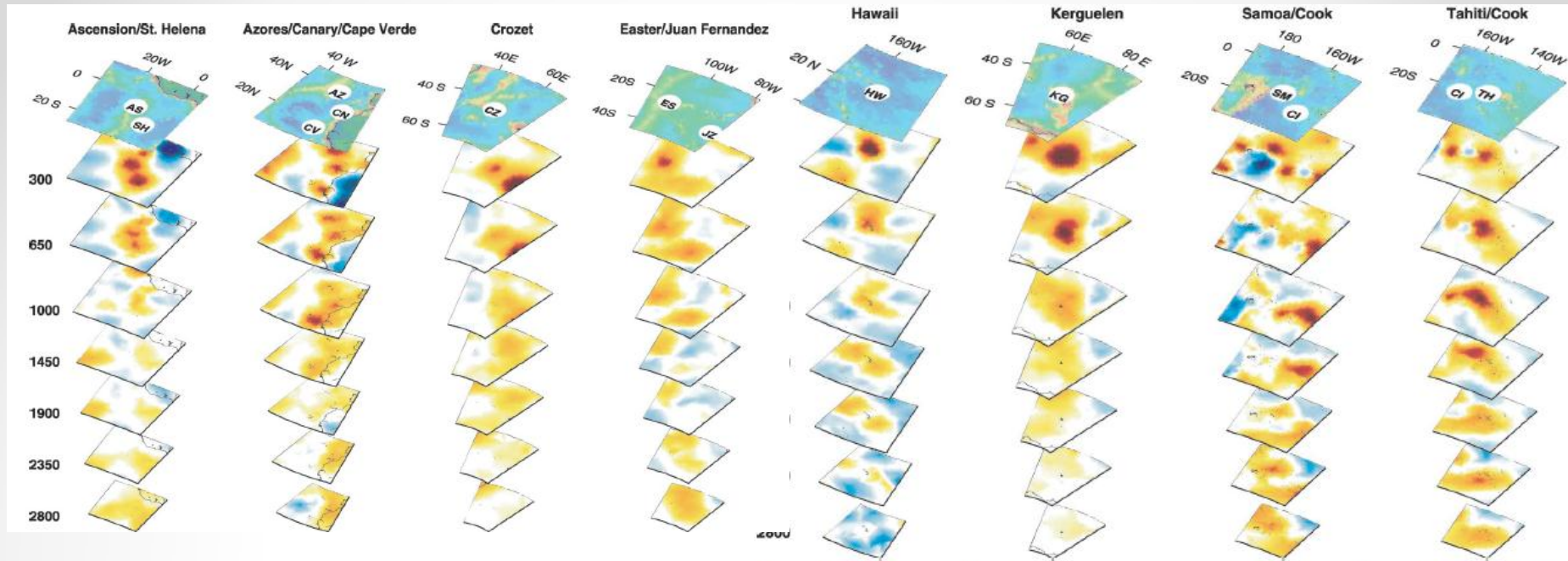


Fig. 2. Three-dimensional view of deep plumes present in our tomographic model. Maps are 40° by 40°, appropriately scaled with depth. Note the vertical exaggeration. The depth spacing changes at 1000 km. The color scale is the same as in Fig. 3. Two-letter identifiers show hotspot locations.

More Hotspots

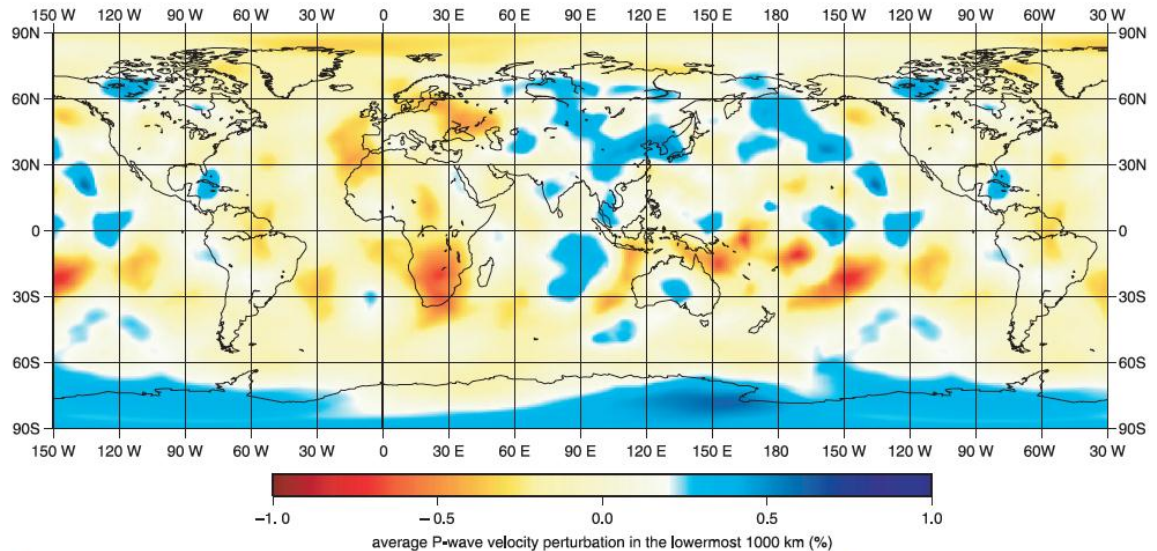
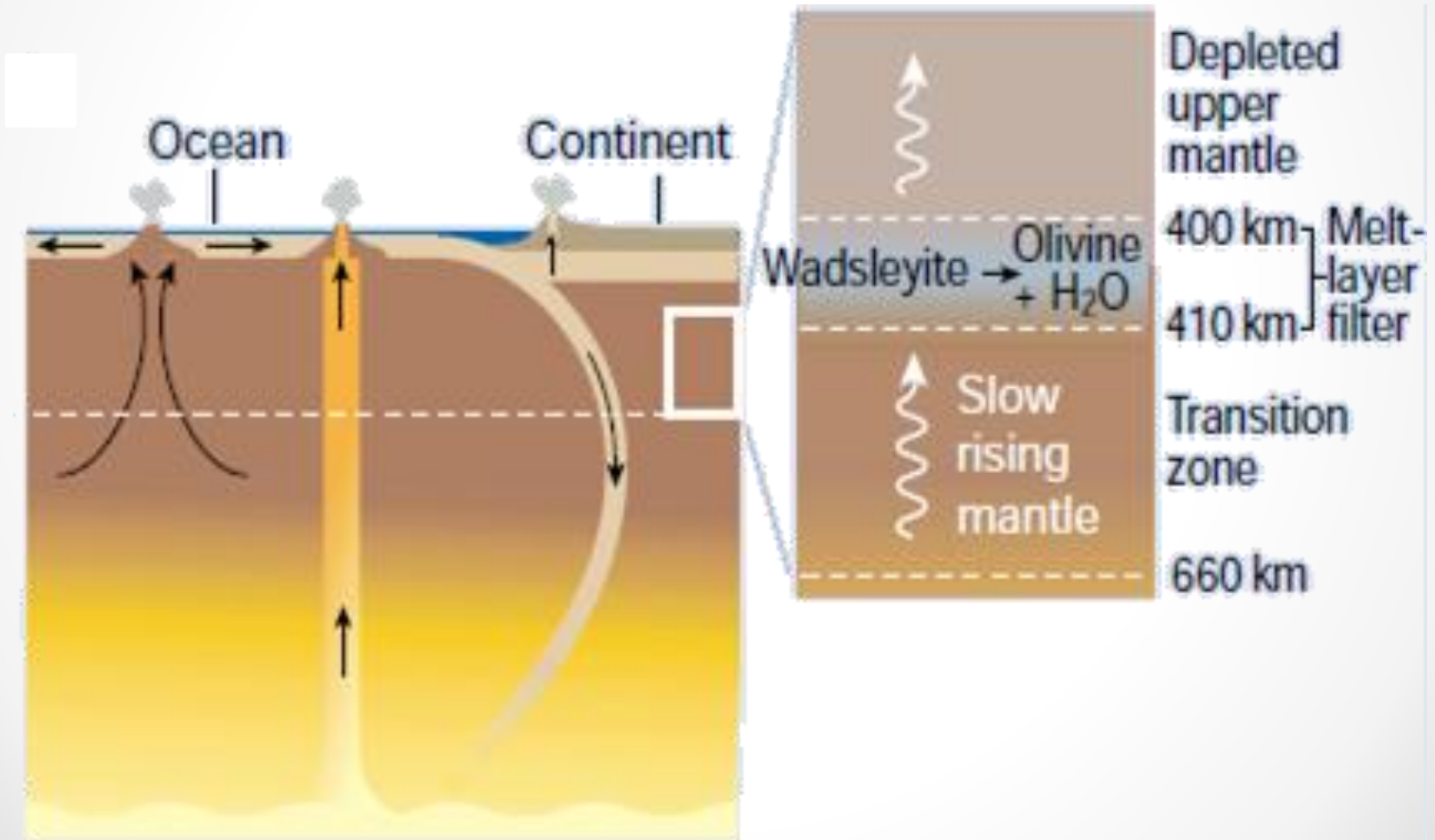


Fig. 1. Vertical average over the lowermost 1000 km of the mantle of the relative velocity perturbation $\delta v_r/v_p$. The averaging emphasizes features that are continuous with depth. Map has been wrapped around to have complete views of both the Atlantic and the Pacific oceans.

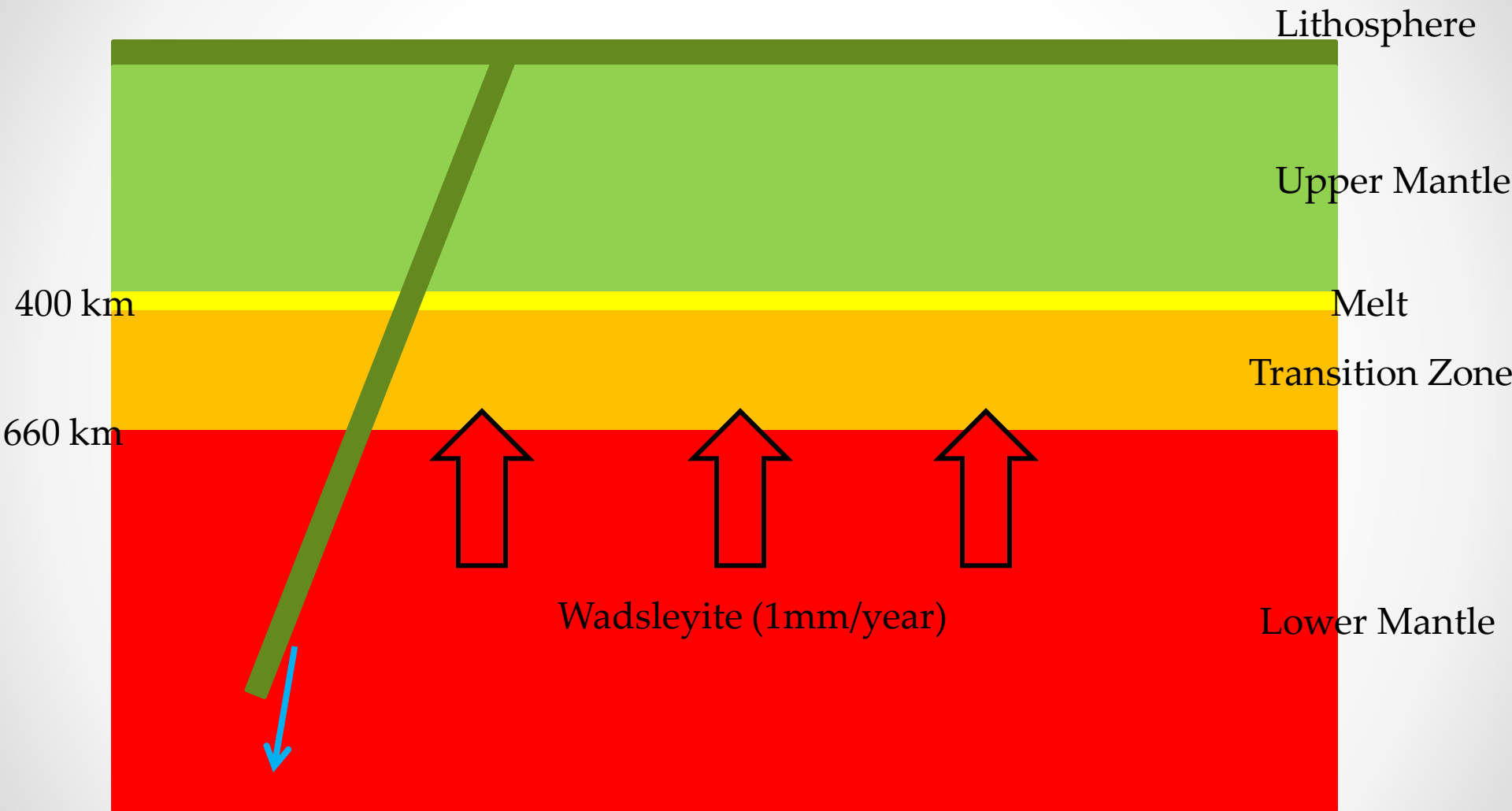
● Montelli et al., 2004

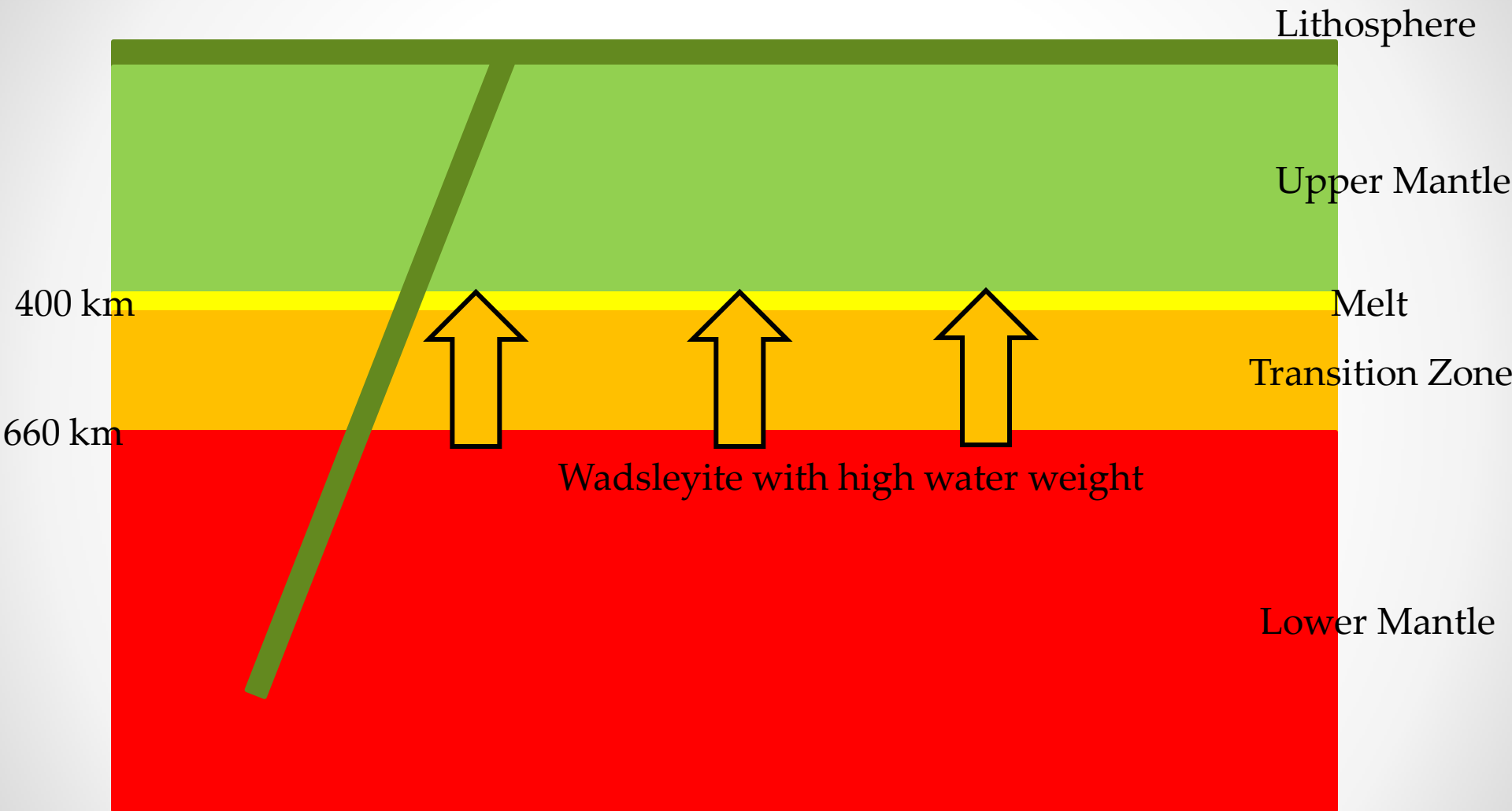
Transition Zone Water Filter

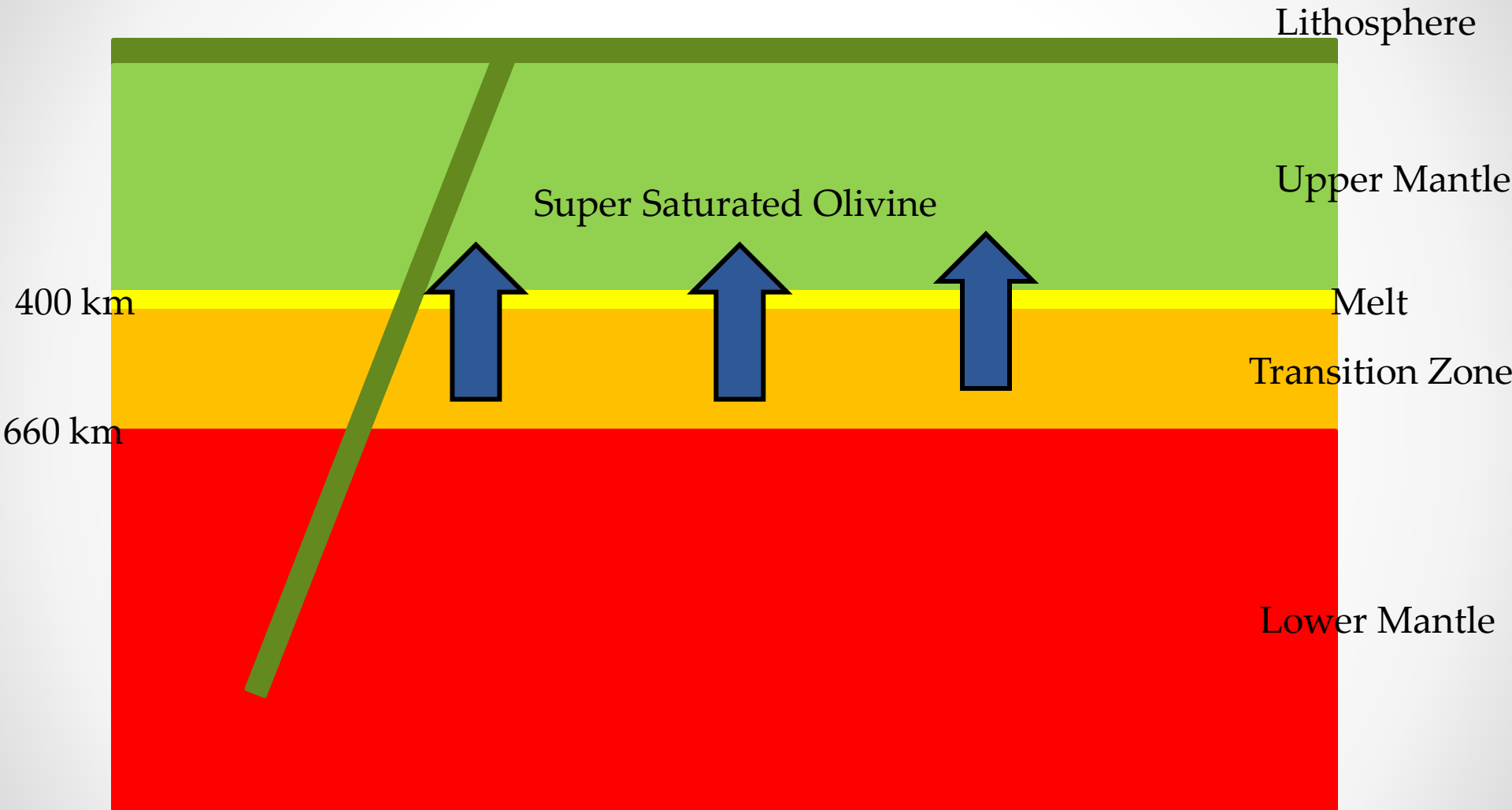


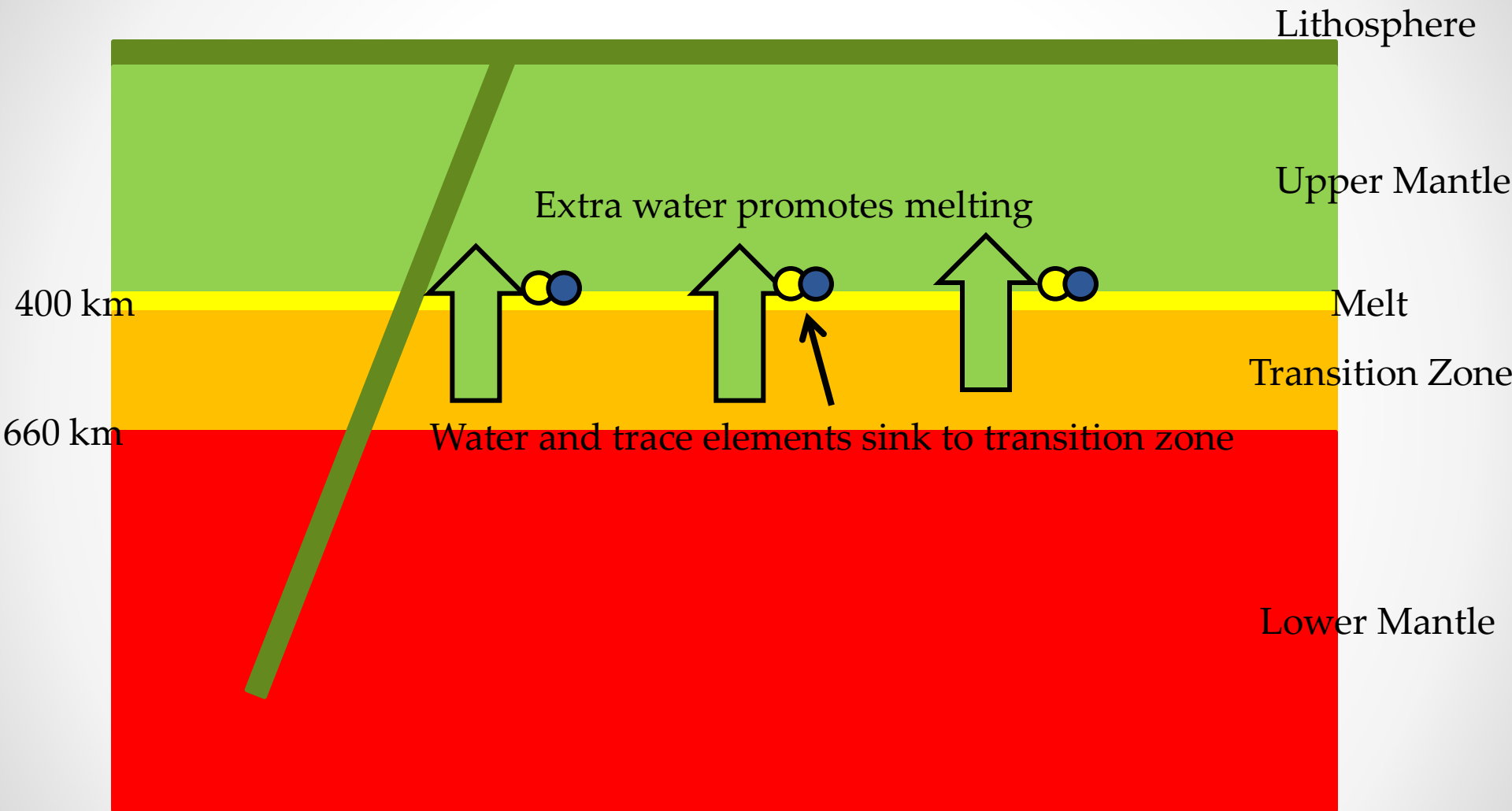
Where's the water at?

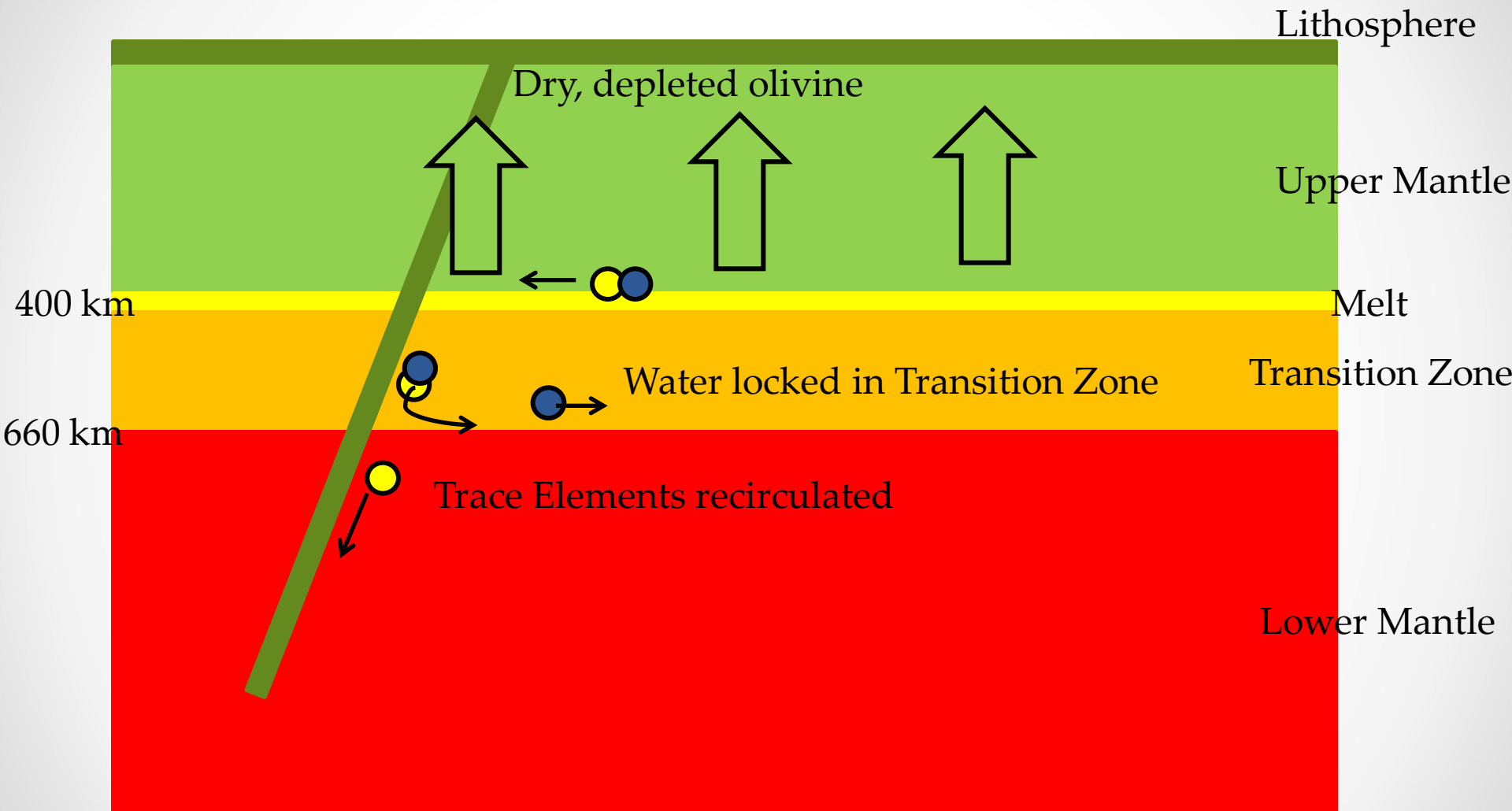
- MORBs → upper mantle is 0.01 wt% water
- OIBs → lower mantle is 0.05 wt% water
- Mantle near subduction zones is 0.1 wt% water
- Water solubility of transition zone minerals → Transition zone is 0.1 – 1.5 wt% water
- Bulk Water estimates → Transition zone is 0.2 – 2% water
- Water weight in transition zone is higher than saturation limit in upper/lower mantle, but lower than saturation limit of transition zone minerals.



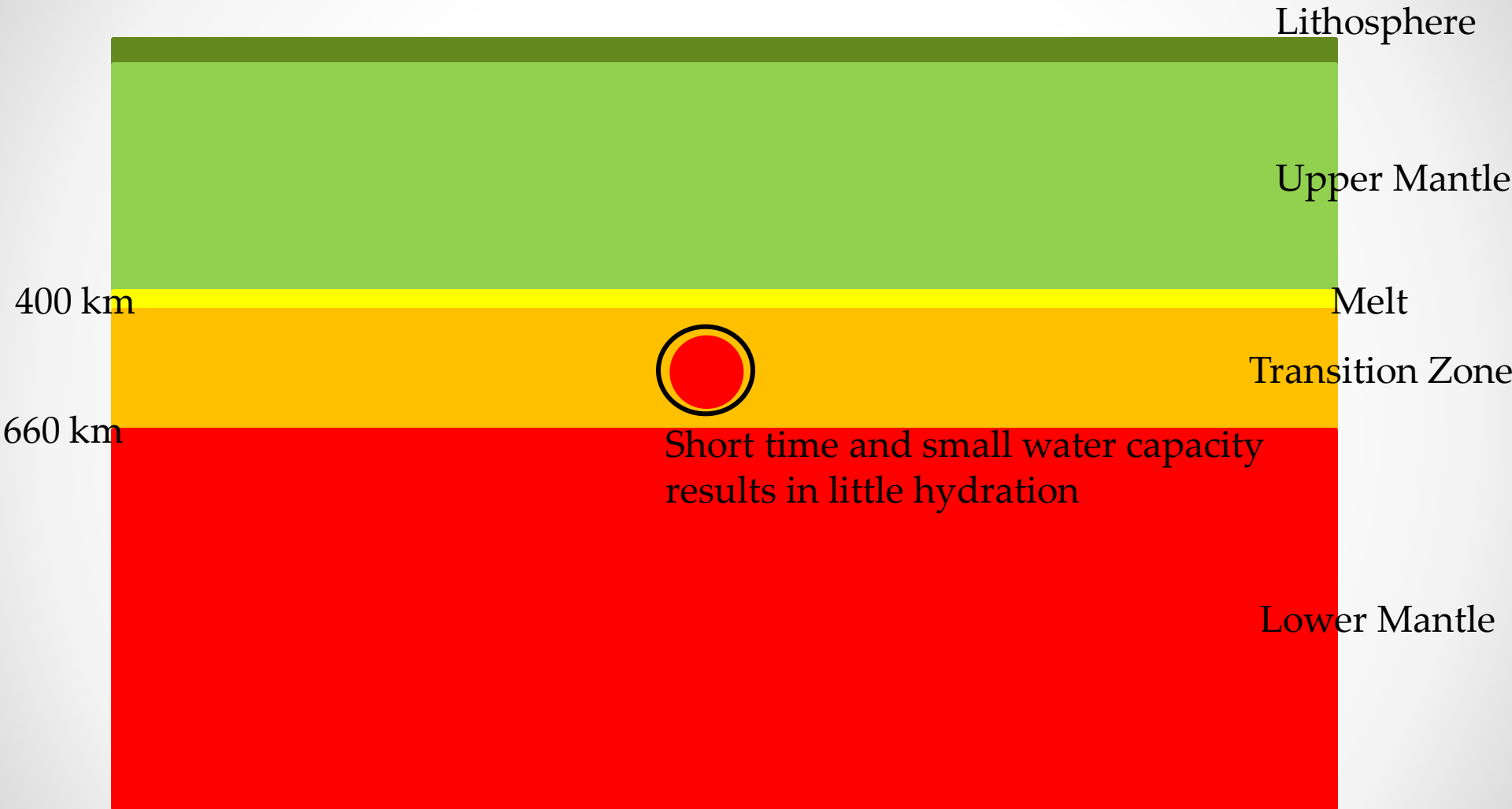


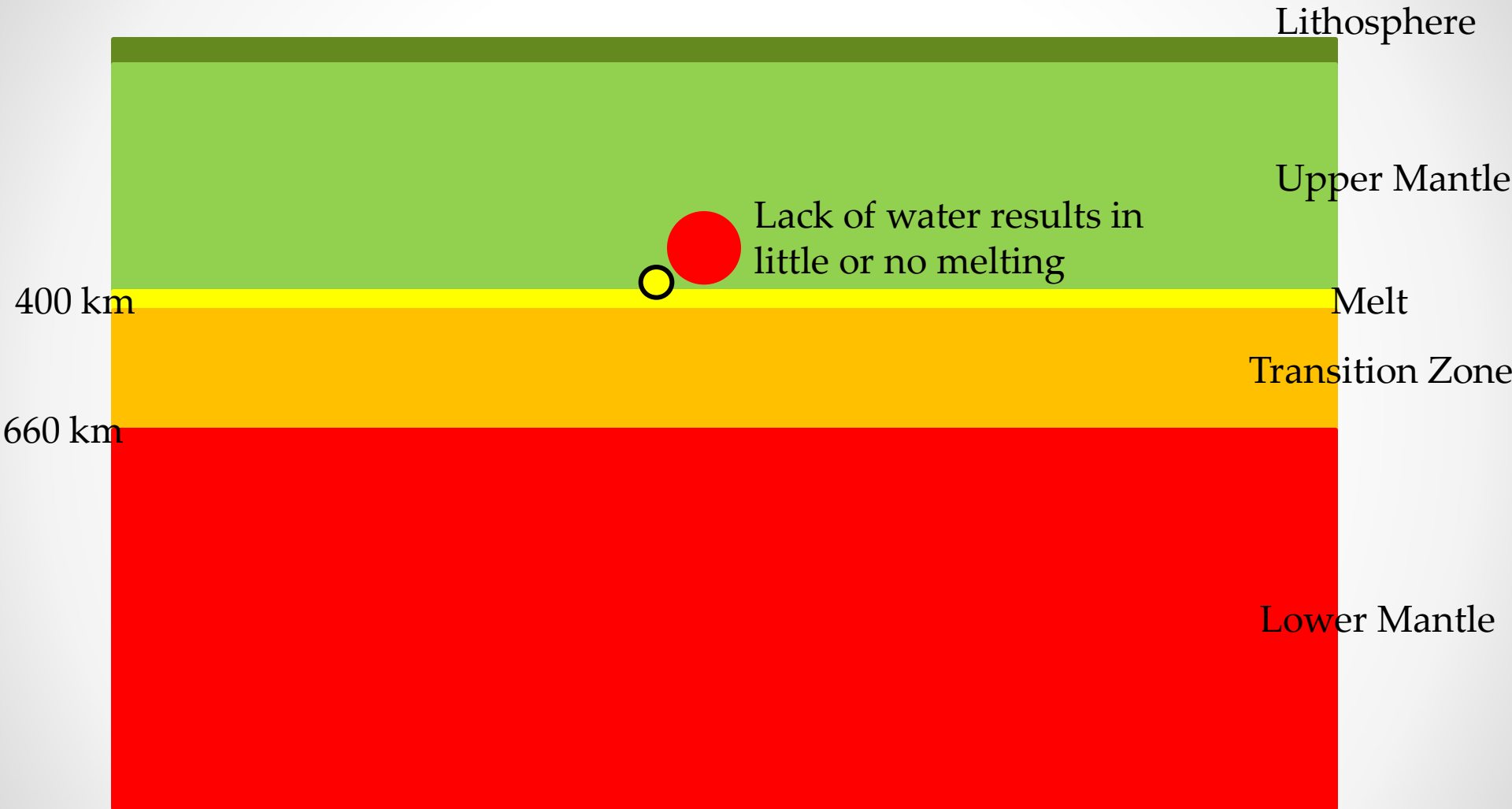












Lithosphere

Upper Mantle

Lack of water results in
little or no melting

400 km

Melt

Transition Zone

660 km

Lower Mantle



Similar story for Archaean mantle resulted in non-depleted crust formation.



Transition Zone Water Filter

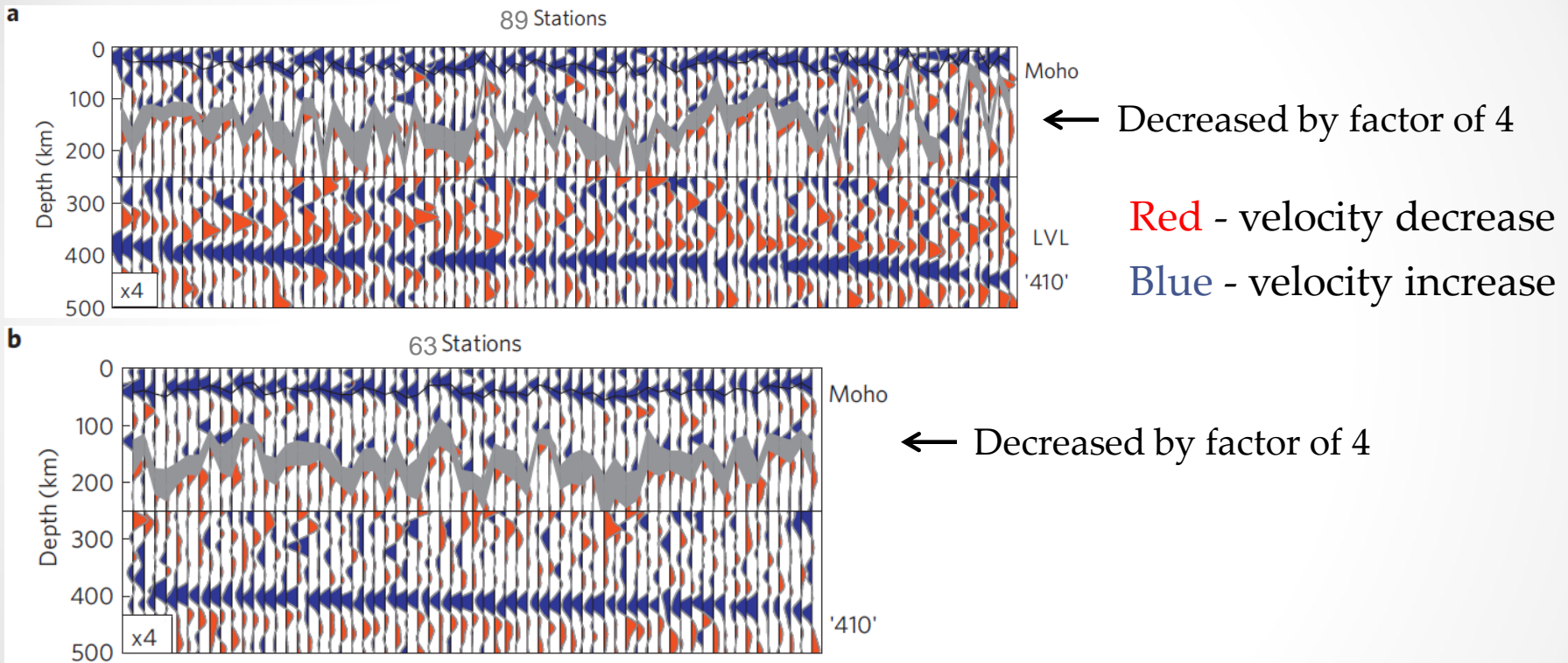
- Heat and silicates are transferred through the whole mantle → whole mantle convection
- “Missing” water is trapped in the transition
- Trace elements are filtered out and only circulate in the lower mantle.

- Melt layer of 5-10 km is hard to image seismically.
- Need better understanding of material properties (i.e. water capacity of mantle rock).



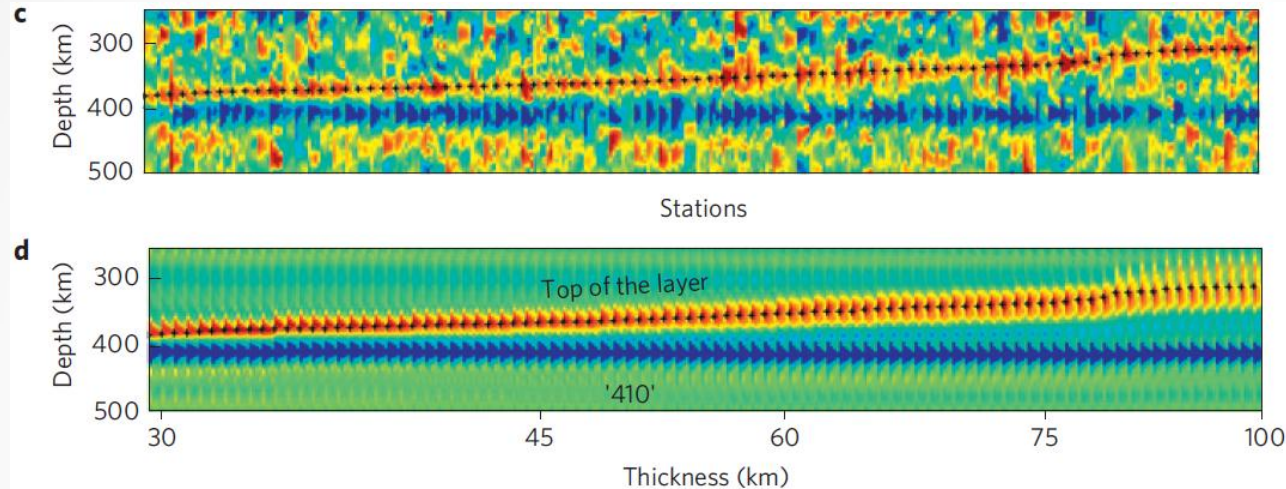
Evidence for Water Filter Theory

Slow velocity layer just above 410-km discontinuity
Data filtered using 4 time periods, with 95% confidence



B. Tauzin, E. Debayle, G. Wittlinger, **Seismic evidence for a global low-velocity layer within the Earth's upper mantle**, *Nature Geoscience* 3, 718–721 (2010)

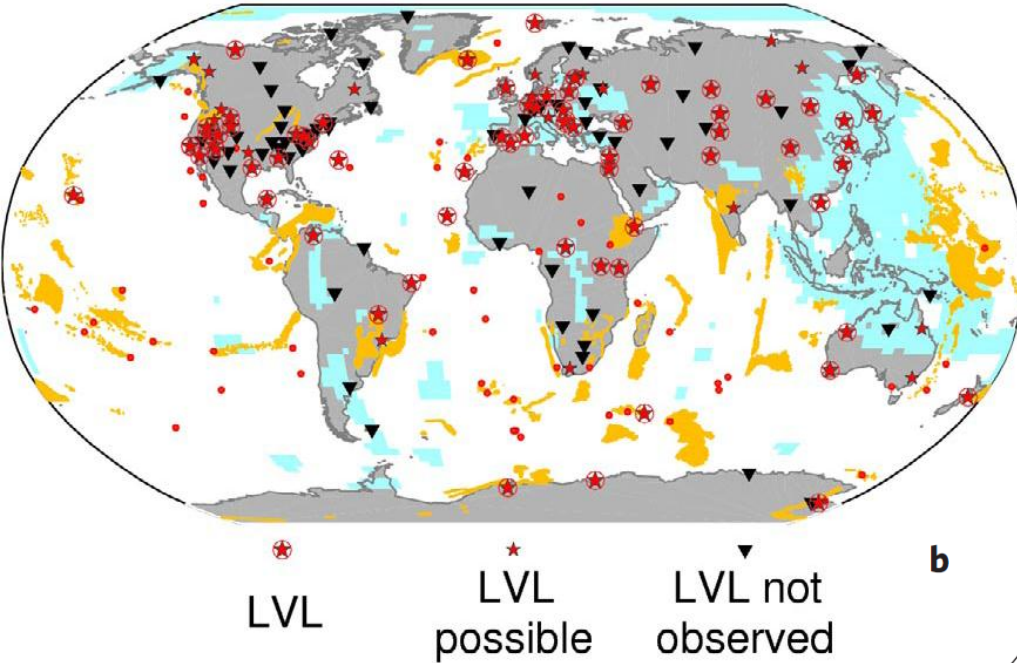
Modeling Receiver Function Observations



c,d, Observed RFs (**c**) for the 89 stations of Fig. 1a and synthetic waveforms (**d**) computed using the same LVL thickness distribution as in the data in **c**. Each seismic trace (**c,d**) is made of the juxtaposition, from left to right, of the 10, 7, 5 and 3 s low-pass filtered RFs at the stations, aligned on the '410' waveform and **ordered by increasing LVL thickness**. Black crosses indicate the top of the LVL.

Sampling and Alternate Explanations

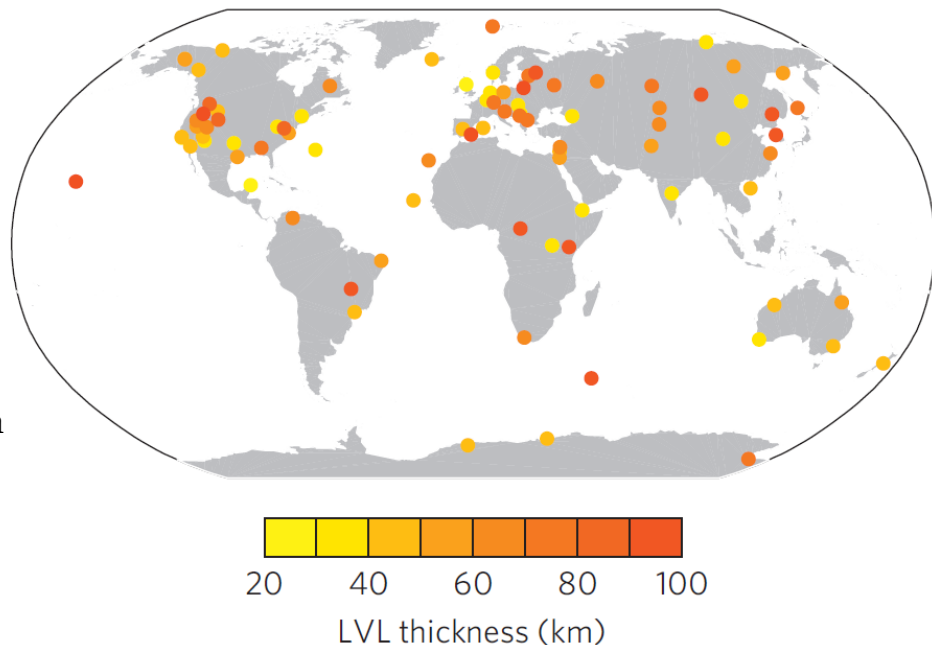
- Igneous provinces
- Subduction zone
- Hotspots



Explanations:

- Few in subduction zones – dehydration
- Few in high temperatures zones - affect water rich mantle silicate rocks
- However, large mantle sampling - it's not solely found in these environments

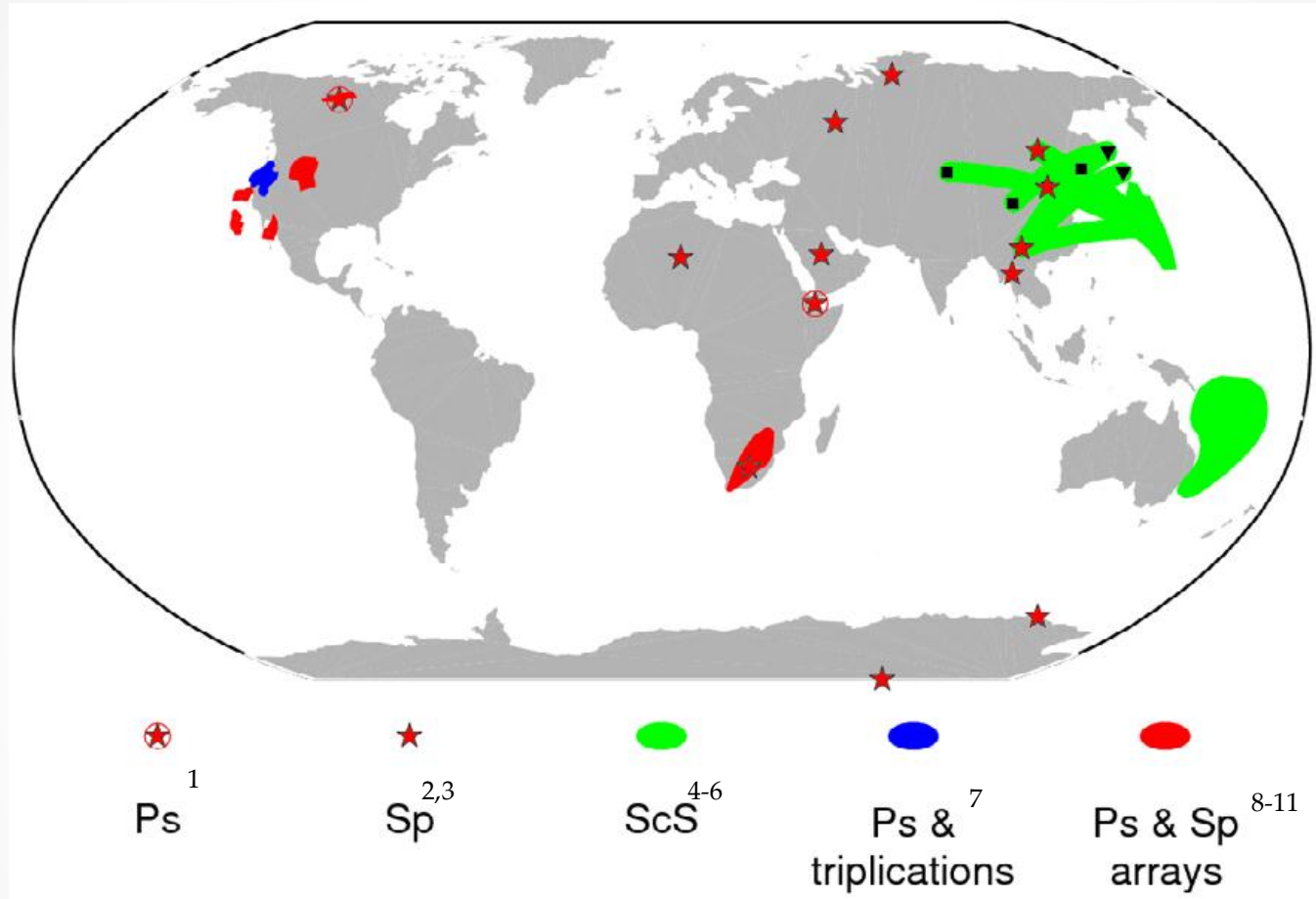
b



Hier-Majumder, S., Ricard, Y. & Bercovici, D. Role of grain boundaries in magma migration and storage. *Earth Planet. Sci. Lett.* 248, 735749 (2006).

- “grain boundary tension may prevent simple gravitational settling of a heavy melt into a thin completely decompacted layer, and may give rise to a thicker boundary layer.”
- This tension is modulated by grain size and matrix viscosity, which can vary by orders of magnitude.

Previous Studies



Former studies showing slow velocity layer above 410-km discontinuity

Summary

- There is clear evidence for slab subduction to the deep mantle
- Theory of water filter above 410-km discontinuity incorporates layered convection-like observations
- Worldwide evidence for thin, slow velocity layer above 410-km discontinuity is emerging

1. Chevrot, S., Vinnik, L. & Montagner, J. P. Global-scale analysis of the mantle P_ds phases. *J. Geophys. Res.* **101**, 20,203-20,219 (1999).
2. Bostock, M. Mantle stratigraphy and evolution of the Slave province. *J. Geophys. Res.* **103**, 21,183-21,200 (1998).
3. Vinnik, L. & Farra, V. Low velocity atop the 410-km discontinuity and mantle plumes. *Earth Planet. Sc. Lett.* **262**, 398-412 (2007).
4. Revenaugh, J. & Sipkin, S. Seismic evidence for silicate melt atop the 410-km discontinuity. *Nature* **369**, 474-476 (1994).
5. Courtier, A. & Revenaugh, J. Deep upper mantle melting beneath the Tasman and the Coral seas detected with multiple ScS reverberations. *Earth Planet. Sc. Lett.* **259**, 66-76 (2007).
6. Bagley, B., Courtier, A. & Revenaugh, J. Melting in the deep upper mantle oceanward of the Honshu slab. *Phys. Earth Planet. Inter.* **175**, 137-144 (2009).
7. Song, T., Helmberger, D. & Grand, S. Low-velocity zone atop the 410-km seismic discontinuity in the northwestern United States. *Nature* **427**, 530-533 (2004).
8. Wittlinger, G. & Farra, V. Converted waves reveal a thick and layered tectosphere beneath the Kalahari super-craton. *Earth Planet. Sc. Lett.* **254**, 404-415 (2007).
9. Jasbinsek, J. & Dueker, K. Ubiquitous low-velocity layer atop the 410-km discontinuity in the northern Rocky Mountains. *Geochem. Geophys. Geosys.* **8**, doi:10.1029/2007GC001661 (2007).
10. Vinnik, L., Ren, Y., Stutzmann, E., Farra, V. & Kiselev, S. Observations of S410p and S350p at seismograph stations in California. *J. Geophys. Res.* **115**, B05303 (2010).
11. Schaeffer, A. J. & Bostock, M. G. A low-velocity zone atop the transition zone in Northwestern Canada. *J. Geophys. Res.* **115**, B06302 (2010).
12. Grand, S., R. van der Hilst, and S. Widiyantoro, Global seismic tomography: A snapshot of convection in the earth, *GSA Today* , **7** , 1-7, (1997).
13. Ren, E. Stutzmann, R.D. van der Hilst, J. Besse Understanding seismic heterogeneities in the lower mantle beneath the Americas from seismic tomography and plate tectonic history *J. Geophys. Res.*, **112** (2007)
14. Lithgow-Bertelloni, M. Richards The dynamics of cenozoic and mesozoic plate motions *Rev. Geophys.*, **36** (1998)
15. Zhao, Global tomographic images of mantle plumes and subducting slabs: insight into deep Earth dynamics, *Phys. Earth Planet. Inter.* **146** (2004).
16. Montelli, G. Nolet, G. Master, F. Dahlen, H. Hung Global P and PP traveltime tomography: rays versus waves *Geophysical Journal International*, **158** 637-654 (2004).